

Spacecraft Attitude and Reaction Wheel Desaturation Combined Control Method

Yaguang Yang*

November 11, 2016

Abstract

Two popular types of spacecraft actuators are reaction wheels and magnetic torque coils. Magnetic torque coils are particularly interesting because they can be used for both attitude control and reaction wheel momentum management (desaturation control). Although these two tasks are performed at the same time using the same set of actuators, most design methods deal with only one of the these tasks or consider these two tasks separately. In this paper, a design with these two tasks in mind is formulated as a single problem. A periodic time-varying linear quadratic regulator design method is then proposed to solve this problem. A simulation example is provided to describe the benefit of the new strategy.

Keywords: Spacecraft attitude control, reaction wheel desaturation, linear time-varying system, reduced quaternion model, linear quadratic regulator.

1 Introduction

Spacecraft attitude control and reaction wheel desaturation are normally regarded as two different control system design problems and are discussed in separate chapters in text books, such as [1, 2]. While spacecraft attitude control using magnetic torques has been one of the main research areas (see, for example, [3, 4] and extensive references therein), there are quite a few research papers that address reaction wheel momentum management, see for example, [5, 6, 7] and references therein. In [5], Dzielsk et al. formulated the problem as an optimization problem and a nonlinear programming method was proposed to find the solution. Their method can be very expensive and there is no guarantee to find the global optimal solution. Chen et al. [6] discussed optimal desaturation controllers using magnetic torques and thrusters. Their methods find the optimal torques which, however, may not be able to achieve by magnetic torque coils because given the desired torques in a three dimensional space, magnetic torque coils can only generate torques in a two dimensional plane [2]. Like most publications on this problem, the above two papers do not consider the time-varying effect of the geomagnetic field in body frame, which arises when a spacecraft flies around the Earth. Giuliatti et al. [7] considered the same problem with more details on the geomagnetic field, but the periodic feature of the magnetic field along the orbit was not used in their proposed design. In addition, all these proposed designs considered only momentum management but not attitude control.

Since both attitude control and reaction wheel desaturation are performed at the same time using the same magnetic torque coils, the control system design should consider these two design objectives at the same time and some very recent research papers tackled the problem in this direction, for example, [8, 9]. In [8], Tregouet et al. studied the problem of the spacecraft stabilization and reaction wheel desaturation at the same time. They considered time-variation of the magnetic field in body frame, and their reference frame was the inertial frame. However, for a Low Earth Orbit (LEO) spacecraft that uses Earth's magnetic field, the reference frame for the spacecraft is most likely Local Vertical Local Horizontal (LVLH) frame. In addition, their design method depends on some assumption which is not easy to verify and their proposed design does not use the periodic feature of the magnetic field. Moreover, their design is composed of two loops, which is essentially an idea of dealing with attitude control and wheel momentum management in separate considerations. In [9], a heuristic proportional controller was proposed and a Lyapunov function was used to prove that the controller can simultaneously stabilize the spacecraft with respect to the LVLH frame and achieve reaction wheel management. But this design method does not consider the the time-varying effect of the geomagnetic field in body frame. Although these two designs are impressive, as we have seen, these designs do not consider some factors in reality and their solutions are not optimal.

In this paper, we propose a more attractive design method which considers as many factors as practical. The controlled attitude is aligned with LVLH frame. A general reduced quaternion model, including (a) reaction wheels, (b) magnetic torque coils, (c) the gravity gradient torque, and (d) the periodic time-varying effects of the geomagnetic field along the orbit and its interaction with magnetic torque coils, is proposed. The model is an extension of the one discussed in [10]. A single objective function, which considers the performance of both attitude control and reaction wheel management at the same time, is suggested. Since a well-designed periodic controller for a period system is better than constant controllers as pointed out in [11, 12], this objective function is optimized using the solution of a matrix periodic Riccati equation described in [13], which leads to a periodic time-varying optimal control. Based on the algorithm for the periodic Riccati equations [13], we show that the design can be calculated in an efficient way and the designed controller is optimal for both the spacecraft attitude control and for the reaction wheel momentum manage at the same time. We provide a simulation test to demonstrate that the designed system achieves more accurate attitude than the optimal control system that uses only magnetic torques. Moreover, the designed controller based on LQR method works on the nonlinear spacecraft system.

The remainder of the paper is organized as follows. Section 2 derives the reduced quaternion spacecraft control system model using reaction wheel and magnetic control torques with the attitude defined as the rotation of the body frame respect to the LVLH frame. Section 3 reduces the nonlinear spacecraft system model to a linearized periodic time-varying model which includes the time-varying geomagnetic field along the orbit, the gravity gradient disturbance torque, the reaction wheel speed control, and the magnetic

torque control. Section 4 introduces a single objective function for both attitude control and wheel management. It also gives the optimal control solutions for this linear time-varying system in different conditions. Simulation test is provided in Section 5. The conclusions are summarized in Section 6.

2 Spacecraft model for attitude and reaction wheel desaturation control

Throughout the discussion, we assume that the inertia matrix of a spacecraft $\mathbf{J} = \text{diag}(J_1, J_2, J_3)$ is a diagonal matrix. This assumption is reasonable because in practical spacecraft design, spacecraft inertia matrix \mathbf{J} is always designed as close to a diagonal matrix as possible [14]. (It is actually very close to a diagonal matrix.) For spacecraft using Earth's magnetic torques, the nadir pointing model is probably the mostly desired one. Therefore, the attitude of the spacecraft is represented by the rotation of the spacecraft body frame relative to the local vertical and local horizontal frame. This means that the quaternion and spacecraft body rate should be represented in terms of the rotation of the spacecraft body frame relative to the LVLH frame (see [14] for the definition of LVLH frame).

Let $\boldsymbol{\omega} = [\omega_1, \omega_2, \omega_3]^T$ be the body rate with respect to the LVLH frame represented in the body frame, $\boldsymbol{\omega}_{lvth} = [0, \omega_0, 0]^T$ the orbit rate (the rotation of LVLH frame) with respect to the inertial frame represented in the LVLH frame¹, and $\boldsymbol{\omega}_I = [\omega_{I1}, \omega_{I2}, \omega_{I3}]^T$ be the angular velocity vector of the spacecraft body with respect to the inertial frame, represented in the spacecraft body frame. Let \mathbf{A}_l^b represent the rotational transformation matrix from the LVLH frame to the spacecraft body frame. Then, $\boldsymbol{\omega}_I$ can be expressed as [10, 14]

$$\boldsymbol{\omega}_I = \boldsymbol{\omega} + \mathbf{A}_l^b \boldsymbol{\omega}_{lvth} = \boldsymbol{\omega} + \boldsymbol{\omega}_{lvth}^b, \quad (1)$$

where $\boldsymbol{\omega}_{lvth}^b$ is the rotational rate of LVLH frame relative to the inertial frame represented in the spacecraft body frame. Assuming that the orbit is circular, i.e., $\dot{\boldsymbol{\omega}}_{lvth} = 0$, using the fact (see [14, eq.(19)])

$$\dot{\mathbf{A}}_l^b = -\boldsymbol{\omega} \times \mathbf{A}_l^b, \quad (2)$$

we have

$$\begin{aligned} \dot{\boldsymbol{\omega}}_I &= \dot{\boldsymbol{\omega}} + \dot{\mathbf{A}}_l^b \boldsymbol{\omega}_{lvth} + \mathbf{A}_l^b \dot{\boldsymbol{\omega}}_{lvth} \\ &= \dot{\boldsymbol{\omega}} - \boldsymbol{\omega} \times \mathbf{A}_l^b \boldsymbol{\omega}_{lvth} = \dot{\boldsymbol{\omega}} - \boldsymbol{\omega} \times \boldsymbol{\omega}_{lvth}^b. \end{aligned} \quad (3)$$

Assuming that the three reaction wheels are aligned with the body frame axes, the total angular momentum of the spacecraft \mathbf{h}_T in the body frame comprises the angular momentum of the spacecraft $\mathbf{J}\boldsymbol{\omega}_I$ and the angular momentum of the reaction wheels $\mathbf{h}_w = [h_{w1}, h_{w2}, h_{w3}]^T$

$$\mathbf{h}_T = \mathbf{J}\boldsymbol{\omega}_I + \mathbf{h}_w, \quad (4)$$

where

$$\mathbf{h}_w = \mathbf{J}_w \boldsymbol{\Omega}, \quad (5)$$

$\mathbf{J}_w = \text{diag}(\mathbf{J}_{w1}, \mathbf{J}_{w2}, \mathbf{J}_{w3})$ is the inertia matrix of the three reaction wheels aligned with the spacecraft body axes, and $\boldsymbol{\Omega} = [\Omega_1, \Omega_2, \Omega_3]^T$ is the angular rate vector of the three reaction wheels. Let \mathbf{h}'_T be the same vector of \mathbf{h}_T represented in inertial frame. Let \mathbf{t}_T be the total external torques acting on the spacecraft, we have (see [15]) $\mathbf{t}_T = \left. \frac{d\mathbf{h}'_T}{dt} \right|_b$. Using eq. (20) of [14] and equation (4), we have the dynamics equations of the spacecraft as follows

$$\begin{aligned} \mathbf{J}\dot{\boldsymbol{\omega}}_I + \dot{\mathbf{h}}_w &= \left. \left(\frac{d\mathbf{h}_T}{dt} \right) \right|_b = -\boldsymbol{\omega}_I \times \mathbf{h}_T + \left. \left(\frac{d\mathbf{h}'_T}{dt} \right) \right|_b \\ &= -\boldsymbol{\omega}_I \times (\mathbf{J}\boldsymbol{\omega}_I + \mathbf{h}_w) + \mathbf{t}_T, \end{aligned} \quad (6)$$

¹ For a circular orbit, given the spacecraft orbital period around the Earth P , $\omega_0 = \frac{2\pi}{P}$ is a known constant.

where \mathbf{t}_T includes the gravity gradient torque \mathbf{t}_g , magnetic control torque \mathbf{t}_m , and internal and external disturbance torque \mathbf{t}_d (including residual magnetic moment induced torque, atmosphere induced torque, solar radiation torque, etc). The torques generated by the reaction wheels \mathbf{t}_w are given by

$$\mathbf{t}_w = \dot{\mathbf{h}}_w = \mathbf{J}_w \dot{\boldsymbol{\Omega}}.$$

Substituting these relations into (6) gives

$$\mathbf{J}\dot{\boldsymbol{\omega}}_I = -\boldsymbol{\omega}_I \times (\mathbf{J}\boldsymbol{\omega}_I + \mathbf{J}_w\boldsymbol{\Omega}) - \mathbf{t}_w + \mathbf{t}_g + \mathbf{t}_m + \mathbf{t}_d. \quad (7)$$

Substituting (1) and (3) into (7), we have

$$\mathbf{J}\dot{\boldsymbol{\omega}} = \mathbf{J}\boldsymbol{\omega} \times \boldsymbol{\omega}_{lvlh}^b - (\boldsymbol{\omega} + \boldsymbol{\omega}_{lvlh}^b) \times [\mathbf{J}(\boldsymbol{\omega} + \boldsymbol{\omega}_{lvlh}^b) + \mathbf{J}_w\boldsymbol{\Omega}] - \mathbf{t}_w + \mathbf{t}_g + \mathbf{t}_m + \mathbf{t}_d. \quad (8)$$

Let

$$\bar{\mathbf{q}} = [q_0, q_1, q_2, q_3]^T = [q_0, \mathbf{q}^T]^T = \left[\cos\left(\frac{\alpha}{2}\right), \hat{\mathbf{e}}^T \sin\left(\frac{\alpha}{2}\right) \right]^T \quad (9)$$

be the quaternion representing the rotation of the body frame relative to the LVLH frame, where $\hat{\mathbf{e}}$ is the unit length rotational axis and α is the rotation angle about $\hat{\mathbf{e}}$. Therefore, the reduced kinematics equation becomes [10]

$$\begin{aligned} \begin{bmatrix} \dot{q}_1 \\ \dot{q}_2 \\ \dot{q}_3 \end{bmatrix} &= \frac{1}{2} \begin{bmatrix} \sqrt{1 - q_1^2 - q_2^2 - q_3^2} & -q_3 & q_2 \\ q_3 & \sqrt{1 - q_1^2 - q_2^2 - q_3^2} & -q_1 \\ -q_2 & q_1 & \sqrt{1 - q_1^2 - q_2^2 - q_3^2} \end{bmatrix} \begin{bmatrix} \omega_1 \\ \omega_2 \\ \omega_3 \end{bmatrix} \\ &= \mathbf{g}(q_1, q_2, q_3, \boldsymbol{\omega}), \end{aligned} \quad (10)$$

or simply

$$\dot{\mathbf{q}} = \mathbf{g}(\mathbf{q}, \boldsymbol{\omega}). \quad (11)$$

Since (see [10, 14]),

$$\mathbf{A}_l^b = \begin{bmatrix} 2q_0^2 - 1 + 2q_1^2 & 2q_1q_2 + 2q_0q_3 & 2q_1q_3 - 2q_0q_2 \\ 2q_1q_2 - 2q_0q_3 & 2q_0^2 - 1 + 2q_2^2 & 2q_2q_3 + 2q_0q_1 \\ 2q_1q_3 + 2q_0q_2 & 2q_2q_3 - 2q_0q_1 & 2q_0^2 - 1 + 2q_3^2 \end{bmatrix},$$

we have

$$\boldsymbol{\omega}_{lvlh}^b = \mathbf{A}_l^b \boldsymbol{\omega}_{lvlh} = \begin{bmatrix} 2q_1q_2 + 2q_0q_3 \\ 2q_0^2 - 1 + 2q_2^2 \\ 2q_2q_3 - 2q_0q_1 \end{bmatrix} \omega_0, \quad (12)$$

which is a function of \mathbf{q} . Interestingly, given spacecraft inertia matrix \mathbf{J} , \mathbf{t}_g is also a function of \mathbf{q} . Using the facts (a) the spacecraft mass is negligible compared to the Earth mass, and (b) the size of the spacecraft is negligible compared to the magnitude of the vector from the center of the Earth to the center of the mass of the spacecraft \mathbf{R} , the gravitational torque is given by [16, page 367]:

$$\mathbf{t}_g = \frac{3\mu}{|\mathbf{R}|^5} \mathbf{R} \times \mathbf{J}\mathbf{R}, \quad (13)$$

where $\mu = GM$, $G = 6.669 * 10^{-11} m^3/kg - s^2$ is the universal constant of gravitation, and M is the mass of the Earth. Noticing that in local vertical local horizontal frame, $\mathbf{R}_l = [0, 0, -|\mathbf{R}|]^T$, we can represent \mathbf{R} in body frame as

$$\mathbf{R} = \mathbf{A}_l^b \mathbf{R}_l = \begin{bmatrix} 2q_0^2 - 1 + 2q_1^2 & 2q_1q_2 + 2q_0q_3 & 2q_1q_3 - 2q_0q_2 \\ 2q_1q_2 - 2q_0q_3 & 2q_0^2 - 1 + 2q_2^2 & 2q_2q_3 + 2q_0q_1 \\ 2q_1q_3 + 2q_0q_2 & 2q_2q_3 - 2q_0q_1 & 2q_0^2 - 1 + 2q_3^2 \end{bmatrix} \begin{bmatrix} 0 \\ 0 \\ -|\mathbf{R}| \end{bmatrix}. \quad (14)$$

Denote the last column of \mathbf{A}_l^b as $\mathbf{A}_l^b(:, 3)$, and using the following relation [2, page 109]

$$\omega_0 = \sqrt{\frac{\mu}{|\mathbf{R}|^3}} \quad (15)$$

and (14), we can rewrite (13) as

$$\mathbf{t}_g = 3\omega_0^2 \mathbf{A}_l^b(:, 3) \times \mathbf{J} \mathbf{A}_l^b(:, 3). \quad (16)$$

Let $\mathbf{b}(t) = [b_1(t), b_2(t), b_3(t)]^T$ be the Earth's magnetic field in the spacecraft coordinates, computed using the spacecraft position, the spacecraft attitude, and a spherical harmonic model of the Earth's magnetic field [1]. Let $\mathbf{m} = [m_1, m_2, m_3]^T$ be the spacecraft magnetic torque coils' induced magnetic moment in the spacecraft coordinates. The desired magnetic control torque \mathbf{t}_m may not be achievable because

$$\mathbf{t}_m = \mathbf{m} \times \mathbf{b} = -\mathbf{b} \times \mathbf{m} \quad (17)$$

provides only a torque in a two dimensional plane but not in the three dimensional space [2]. However, the spacecraft magnetic torque coils' induced magnetic moment \mathbf{m} is an achievable engineering variable. Therefore, equation (8) should be rewritten as

$$\mathbf{J}\dot{\boldsymbol{\omega}} = \mathbf{f}(\boldsymbol{\omega}, \boldsymbol{\Omega}, \mathbf{q}) - \mathbf{t}_w + \mathbf{t}_g - \mathbf{b} \times \mathbf{m} + \mathbf{t}_d, \quad (18)$$

where

$$\mathbf{f}(\boldsymbol{\omega}, \boldsymbol{\Omega}, \mathbf{q}) = \mathbf{J}\boldsymbol{\omega} \times \boldsymbol{\omega}_{lvlh}^b - (\boldsymbol{\omega} + \boldsymbol{\omega}_{lvlh}^b) \times [\mathbf{J}(\boldsymbol{\omega} + \boldsymbol{\omega}_{lvlh}^b) + \mathbf{J}_w \boldsymbol{\Omega}]. \quad (19)$$

Notice that the cross product of $\mathbf{b} \times \mathbf{m}$ can be expressed as product of an asymmetric matrix \mathbf{b}^\times and the vector \mathbf{m} with

$$\mathbf{b}^\times = \begin{bmatrix} 0 & -b_3 & b_2 \\ b_3 & 0 & -b_1 \\ -b_2 & b_1 & 0 \end{bmatrix}. \quad (20)$$

Denote the system states $\mathbf{x} = [\boldsymbol{\omega}^T, \boldsymbol{\Omega}^T, \mathbf{q}^T]^T$ and control inputs $\mathbf{u} = [\mathbf{t}_w^T, \mathbf{m}^T]^T$, the spacecraft control system model can be written as follows:

$$\mathbf{J}\dot{\boldsymbol{\omega}} = \mathbf{f}(\boldsymbol{\omega}, \boldsymbol{\Omega}, \mathbf{q}) + \mathbf{t}_g - [\mathbf{I}, \mathbf{b}^\times] \mathbf{u} + \mathbf{t}_d, \quad (21a)$$

$$\mathbf{J}_w \dot{\boldsymbol{\Omega}} = \mathbf{t}_w, \quad (21b)$$

$$\dot{\mathbf{q}} = \mathbf{g}(\mathbf{q}, \boldsymbol{\omega}). \quad (21c)$$

Remark 2.1 *The reduced quaternion, instead of the full quaternion, is proposed in this model because of many merits discussed in [10, 17, 18].*

3 Linearized model for attitude and reaction wheel desaturation control

The nonlinear model of (21) can be used to design control systems. One popular design method for nonlinear model involves Lyapunov stability theorem, which is actually used in [8, 9]. A design based on this method focuses on stability but not on performance. Another widely known method is nonlinear optimal control design [5], it normally produces an open loop controller which is not robust [19] and its computational cost is high. Therefore, We propose to use Linear Quadratic Regulator (LQR) which achieves the optimal performance for the linearized system and is a closed-loop feedback control. Our task in this section is to derive the linearized model for the nonlinear system (21).

Using the linearization technique of [10, 14], we can express $\boldsymbol{\omega}_{lvlh}^b$ in (12) approximately as a linear function of \mathbf{q} as follows

$$\boldsymbol{\omega}_{lvlh}^b \approx \begin{bmatrix} 2q_3 \\ 1 \\ -2q_1 \end{bmatrix} \omega_0 = \begin{bmatrix} 0 & 0 & 2\omega_0 \\ 0 & 0 & 0 \\ -2\omega_0 & 0 & 0 \end{bmatrix} \mathbf{q} + \begin{bmatrix} 0 \\ \omega_0 \\ 0 \end{bmatrix}. \quad (22)$$

Similarly, we can express \mathbf{t}_g in (16) approximately as a linear function of \mathbf{q} as follows

$$\mathbf{t}_g \approx \begin{bmatrix} 6\omega_0^2(J_3 - J_2)q_1 \\ 6\omega_0^2(J_3 - J_1)q_2 \\ 0 \end{bmatrix} = \begin{bmatrix} 6\omega_0^2(J_3 - J_2) & 0 & 0 \\ 0 & 6\omega_0^2(J_3 - J_1) & 0 \\ 0 & 0 & 0 \end{bmatrix} \mathbf{q} := \mathbf{T}\mathbf{q}. \quad (23)$$

Since \mathbf{t}_g and $\boldsymbol{\omega}_{lvlh}^b$ are functions of \mathbf{q} , the linearized spacecraft model can be expressed as follows:

$$\begin{bmatrix} \mathbf{J} & \mathbf{0} & \mathbf{0} \\ \mathbf{0} & \mathbf{J}_w & \mathbf{0} \\ \mathbf{0} & \mathbf{0} & \mathbf{I} \end{bmatrix} \begin{bmatrix} \dot{\boldsymbol{\omega}} \\ \dot{\boldsymbol{\Omega}} \\ \dot{\mathbf{q}} \end{bmatrix} = \begin{bmatrix} \frac{\partial \mathbf{f}}{\partial \boldsymbol{\omega}} & \frac{\partial \mathbf{f}}{\partial \boldsymbol{\Omega}} & \frac{\partial \mathbf{f}}{\partial \mathbf{q}} + \mathbf{T} \\ \mathbf{0} & \mathbf{0} & \mathbf{0} \\ \frac{\partial \mathbf{g}}{\partial \boldsymbol{\omega}} & \mathbf{0} & \frac{\partial \mathbf{g}}{\partial \mathbf{q}} \end{bmatrix} \begin{bmatrix} \boldsymbol{\omega} \\ \boldsymbol{\Omega} \\ \mathbf{q} \end{bmatrix} + \begin{bmatrix} -\mathbf{I} & -\mathbf{b}^\times \\ \mathbf{I} & \mathbf{0} \\ \mathbf{0} & \mathbf{0} \end{bmatrix} \begin{bmatrix} \mathbf{t}_w \\ \mathbf{m} \end{bmatrix} + \begin{bmatrix} \mathbf{t}_d \\ \mathbf{0} \\ \mathbf{0} \end{bmatrix}, \quad (24)$$

where $\frac{\partial \mathbf{f}}{\partial \boldsymbol{\omega}}$, $\frac{\partial \mathbf{f}}{\partial \boldsymbol{\Omega}}$, $\frac{\partial \mathbf{f}}{\partial \mathbf{q}}$, $\frac{\partial \mathbf{g}}{\partial \boldsymbol{\omega}}$, and $\frac{\partial \mathbf{g}}{\partial \mathbf{q}}$ are evaluated at the desired equilibrium point $\boldsymbol{\omega} = \mathbf{0}$, $\boldsymbol{\Omega} = \mathbf{0}$, and $\mathbf{q} = \mathbf{0}$. Using the definition of (20), (22), (23), and (19), we have

$$\begin{aligned} \left. \frac{\partial \mathbf{f}}{\partial \boldsymbol{\omega}} \right|_{\substack{\boldsymbol{\omega} \approx \mathbf{0} \\ \boldsymbol{\Omega} \approx \mathbf{0} \\ \mathbf{q} \approx \mathbf{0}}} &\approx -\mathbf{J}(\boldsymbol{\omega}_{lvlh}^b)^\times + (\mathbf{J}\boldsymbol{\omega}_{lvlh}^b)^\times - (\boldsymbol{\omega}_{lvlh}^b)^\times \mathbf{J} \Big|_{\substack{\boldsymbol{\omega} \approx \mathbf{0} \\ \boldsymbol{\Omega} \approx \mathbf{0} \\ \mathbf{q} \approx \mathbf{0}}} \\ &= -\mathbf{J} \begin{bmatrix} 0 & 0 & \omega_0 \\ 0 & 0 & 0 \\ -\omega_0 & 0 & 0 \end{bmatrix} + \begin{bmatrix} 0 & 0 & J_2\omega_0 \\ 0 & 0 & 0 \\ -J_2\omega_0 & 0 & 0 \end{bmatrix} - \begin{bmatrix} 0 & 0 & \omega_0 \\ 0 & 0 & 0 \\ -\omega_0 & 0 & 0 \end{bmatrix} \mathbf{J} \\ &= \begin{bmatrix} 0 & 0 & \omega_0(-J_1 + J_2 - J_3) \\ 0 & 0 & 0 \\ \omega_0(J_1 - J_2 + J_3) & 0 & 0 \end{bmatrix}, \end{aligned} \quad (25)$$

$$\begin{aligned} \left. \frac{\partial \mathbf{f}}{\partial \boldsymbol{\Omega}} \right|_{\substack{\boldsymbol{\omega} \approx \mathbf{0} \\ \boldsymbol{\Omega} \approx \mathbf{0} \\ \mathbf{q} \approx \mathbf{0}}} &\approx -(\boldsymbol{\omega})^\times \mathbf{J}_w - (\boldsymbol{\omega}_{lvlh}^b)^\times \mathbf{J}_w \Big|_{\substack{\boldsymbol{\omega} \approx \mathbf{0} \\ \boldsymbol{\Omega} \approx \mathbf{0} \\ \mathbf{q} \approx \mathbf{0}}} = - \begin{bmatrix} 0 & 0 & \omega_0 \\ 0 & 0 & 0 \\ -\omega_0 & 0 & 0 \end{bmatrix} \mathbf{J}_w \\ &= \begin{bmatrix} 0 & 0 & -\omega_0 J_{w3} \\ 0 & 0 & 0 \\ \omega_0 J_{w1} & 0 & 0 \end{bmatrix}, \end{aligned} \quad (26)$$

and

$$\begin{aligned} \left. \frac{\partial \mathbf{f}}{\partial \mathbf{q}} \right|_{\substack{\boldsymbol{\omega} \approx \mathbf{0} \\ \boldsymbol{\Omega} \approx \mathbf{0} \\ \mathbf{q} \approx \mathbf{0}}} &\approx -\frac{\partial}{\partial \mathbf{q}} (\boldsymbol{\omega}_{lvlh}^b \times \mathbf{J}\boldsymbol{\omega}_{lvlh}^b) \Big|_{\substack{\boldsymbol{\omega} \approx \mathbf{0} \\ \boldsymbol{\Omega} \approx \mathbf{0} \\ \mathbf{q} \approx \mathbf{0}}} \\ &\approx (\mathbf{J}\boldsymbol{\omega}_{lvlh}^b)^\times \begin{bmatrix} 0 & 0 & 2\omega_0 \\ 0 & 0 & 0 \\ -2\omega_0 & 0 & 0 \end{bmatrix} - (\boldsymbol{\omega}_{lvlh}^b)^\times \mathbf{J} \begin{bmatrix} 0 & 0 & 2\omega_0 \\ 0 & 0 & 0 \\ -2\omega_0 & 0 & 0 \end{bmatrix} \\ &\approx \omega_0 \left(\begin{bmatrix} 2J_1q_3 \\ J_2 \\ -2J_3q_1 \end{bmatrix}^\times - \begin{bmatrix} 0 & 0 & 1 \\ 0 & 0 & 0 \\ -1 & 0 & 0 \end{bmatrix} \mathbf{J} \right) \begin{bmatrix} 0 & 0 & 2\omega_0 \\ 0 & 0 & 0 \\ -2\omega_0 & 0 & 0 \end{bmatrix} \\ &\approx \omega_0 \begin{bmatrix} 0 & 0 & J_2 - J_3 \\ 0 & 0 & 0 \\ J_1 - J_2 & 0 & 0 \end{bmatrix} \begin{bmatrix} 0 & 0 & 2\omega_0 \\ 0 & 0 & 0 \\ -2\omega_0 & 0 & 0 \end{bmatrix} \\ &= \begin{bmatrix} 2\omega_0^2(J_3 - J_2) & 0 & 0 \\ 0 & 0 & 0 \\ 0 & 0 & 2\omega_0^2(J_1 - J_2) \end{bmatrix}. \end{aligned} \quad (27)$$

From (11), we have

$$\left. \frac{\partial \mathbf{g}}{\partial \boldsymbol{\omega}} \right|_{\substack{\boldsymbol{\omega} \approx \mathbf{0} \\ \mathbf{q} \approx \mathbf{0}}} \approx \frac{1}{2} \mathbf{I}, \quad (28)$$

$$\left. \frac{\partial \mathbf{g}}{\partial \mathbf{q}} \right|_{\substack{\omega \approx 0 \\ \mathbf{q} \approx 0}} \approx \mathbf{0}. \quad (29)$$

Substituting (23), (20), (25), (26), (27), (28), and (29) into (24), we have

$$\begin{aligned} \begin{bmatrix} \dot{\omega} \\ \dot{\Omega} \\ \dot{\mathbf{q}} \end{bmatrix} &= \begin{bmatrix} \mathbf{J}^{-1} \frac{\partial \mathbf{f}}{\partial \omega} & \mathbf{J}^{-1} \frac{\partial \mathbf{f}}{\partial \Omega} & \mathbf{J}^{-1} \left(\frac{\partial \mathbf{f}}{\partial \mathbf{q}} + \mathbf{T} \right) \\ \mathbf{0} & \mathbf{0} & \mathbf{0} \\ \frac{\partial \mathbf{g}}{\partial \omega} & \mathbf{0} & \frac{\partial \mathbf{g}}{\partial \mathbf{q}} \end{bmatrix} \begin{bmatrix} \omega \\ \Omega \\ \mathbf{q} \end{bmatrix} + \begin{bmatrix} -\mathbf{J}^{-1} & -\mathbf{J}^{-1} \mathbf{b}^\times \\ \mathbf{J}_w^{-1} & \mathbf{0} \\ \mathbf{0} & \mathbf{0} \end{bmatrix} \begin{bmatrix} t_w \\ \mathbf{m} \end{bmatrix} + \begin{bmatrix} \mathbf{J}^{-1} \\ \mathbf{0} \\ \mathbf{0} \end{bmatrix} t_d \\ &= \begin{bmatrix} 0 & 0 & \omega_0 \frac{J_1 - J_2 + J_3}{-J_1} & 0 & 0 & \frac{\omega_0 J_{w_3}}{-J_1} & 8\omega_0^2 \frac{J_3 - J_2}{J_1} & 0 & 0 \\ 0 & 0 & 0 & 0 & 0 & 0 & 0 & 6\omega_0^2 \frac{J_3 - J_1}{J_2} & 0 \\ \omega_0 \frac{J_1 - J_2 + J_3}{J_3} & 0 & 0 & \frac{\omega_0 J_{w_1}}{J_3} & 0 & 0 & 0 & 0 & 2\omega_0^2 \frac{J_1 - J_2}{J_3} \\ 0 & 0 & 0 & 0 & 0 & 0 & 0 & 0 & 0 \\ 0 & 0 & 0 & 0 & 0 & 0 & 0 & 0 & 0 \\ 0 & 0 & 0 & 0 & 0 & 0 & 0 & 0 & 0 \\ 0.5 & 0 & 0 & 0 & 0 & 0 & 0 & 0 & 0 \\ 0 & 0.5 & 0 & 0 & 0 & 0 & 0 & 0 & 0 \\ 0 & 0 & 0.5 & 0 & 0 & 0 & 0 & 0 & 0 \end{bmatrix} \begin{bmatrix} \omega_1 \\ \omega_2 \\ \omega_3 \\ \Omega_1 \\ \Omega_2 \\ \Omega_3 \\ q_1 \\ q_2 \\ q_3 \end{bmatrix} \\ &+ \begin{bmatrix} -J_1^{-1} & 0 & 0 & 0 & \frac{b_3}{J_1} & -\frac{b_2}{J_1} \\ 0 & -J_2^{-1} & 0 & -\frac{b_3}{J_2} & 0 & \frac{b_1}{J_2} \\ 0 & 0 & -J_3^{-1} & \frac{b_2}{J_3} & -\frac{b_1}{J_3} & 0 \\ J_{w_1}^{-1} & 0 & 0 & 0 & 0 & 0 \\ 0 & J_{w_2}^{-1} & 0 & 0 & 0 & 0 \\ 0 & 0 & J_{w_3}^{-1} & 0 & 0 & 0 \\ 0 & 0 & 0 & 0 & 0 & 0 \\ 0 & 0 & 0 & 0 & 0 & 0 \\ 0 & 0 & 0 & 0 & 0 & 0 \end{bmatrix} \begin{bmatrix} t_{w_1} \\ t_{w_1} \\ t_{w_1} \\ m_1 \\ m_2 \\ m_3 \end{bmatrix} + \begin{bmatrix} t_{d_1}/J_1 \\ t_{d_2}/J_2 \\ t_{d_3}/J_3 \\ 0 \\ 0 \\ 0 \\ 0 \\ 0 \\ 0 \end{bmatrix} := \mathbf{Ax} + \mathbf{Bu} + \mathbf{d}. \quad (30) \end{aligned}$$

It is worthwhile to notice that (30) is in general a time-varying system. The time-variation of the system arises from an approximately periodic function of $\mathbf{b}(t) = \mathbf{b}(t + P)$, where

$$P = \frac{2\pi}{\omega_0} = 2\pi \sqrt{\frac{a^3}{GM}} \quad (31)$$

is the orbital period, a is the orbital radius (approximately equal to the spacecraft altitude plus the radius of the Earth), and $GM = 3.986005 * 10^{14} m^3/s^2$ [1]. This magnetic field $\mathbf{b}(t)$ can be approximately expressed as follows [20]:

$$\begin{bmatrix} b_1(t) \\ b_2(t) \\ b_3(t) \end{bmatrix} = \frac{\mu_f}{a^3} \begin{bmatrix} \cos(\omega_0 t) \sin(i_m) \\ -\cos(i_m) \\ 2 \sin(\omega_0 t) \sin(i_m) \end{bmatrix}, \quad (32)$$

where i_m is the inclination of the spacecraft orbit with respect to the magnetic equator, $\mu_f = 7.9 \times 10^{15}$ Wb-m is the field's dipole strength. The time $t = 0$ is measured at the ascending-node crossing of the magnetic equator. Therefore, the periodic time-varying matrix \mathbf{B} in (30) can be written as

$$\mathbf{B} = \begin{bmatrix} -J_1^{-1} & 0 & 0 & 0 & \frac{2\mu_f}{a^3 J_1} \sin(i_m) \sin(\omega_0 t) & \frac{\mu_f}{a^3 J_1} \cos(i_m) \\ 0 & -J_2^{-1} & 0 & -\frac{2\mu_f}{a^3 J_2} \sin(i_m) \sin(\omega_0 t) & 0 & \frac{\mu_f}{a^3 J_2} \sin(i_m) \cos(\omega_0 t) \\ 0 & 0 & -J_3^{-1} & -\frac{\mu_f}{a^3 J_3} \cos(i_m) & -\frac{\mu_f}{a^3 J_3} \sin(i_m) \cos(\omega_0 t) & 0 \\ J_{w_1}^{-1} & 0 & 0 & 0 & 0 & 0 \\ 0 & J_{w_2}^{-1} & 0 & 0 & 0 & 0 \\ 0 & 0 & J_{w_3}^{-1} & 0 & 0 & 0 \\ 0 & 0 & 0 & 0 & 0 & 0 \\ 0 & 0 & 0 & 0 & 0 & 0 \\ 0 & 0 & 0 & 0 & 0 & 0 \end{bmatrix}. \quad (33)$$

A special case is when $i_m = 0$, i.e., the spacecraft orbit is on the equator plane of the Earth's magnetic field. In this case, $\mathbf{b}(t) = [0, -\frac{\mu_f}{a^3}, 0]^T$ is a constant vector and \mathbf{B} is reduced to a constant matrix given as follows:

$$\mathbf{B} = \begin{bmatrix} -J_1^{-1} & 0 & 0 & 0 & 0 & \frac{\mu_f}{a^3 J_1} \\ 0 & -J_2^{-1} & 0 & 0 & 0 & 0 \\ 0 & 0 & -J_3^{-1} & -\frac{\mu_f}{a^3 J_3} & 0 & 0 \\ J_{w_1}^{-1} & 0 & 0 & 0 & 0 & 0 \\ 0 & J_{w_2}^{-1} & 0 & 0 & 0 & 0 \\ 0 & 0 & J_{w_3}^{-1} & 0 & 0 & 0 \\ 0 & 0 & 0 & 0 & 0 & 0 \\ 0 & 0 & 0 & 0 & 0 & 0 \\ 0 & 0 & 0 & 0 & 0 & 0 \end{bmatrix}. \quad (34)$$

In the remainder of the discussion, we will consider the discrete time system of (30) because it is more suitable for computer controlled system implementations. The discrete time system is given as follows:

$$\mathbf{x}_{k+1} = \mathbf{A}\mathbf{x}_k + \mathbf{B}_k\mathbf{u}_k + \mathbf{d}_k. \quad (35)$$

Assuming the sampling time is t_s , the simplest but less accurate discretization formulas to get \mathbf{A}_k and \mathbf{B}_k are given as follows:

$$\mathbf{A}_k = (\mathbf{I} + t_s\mathbf{A}), \quad \mathbf{B}_k = t_s\mathbf{B}(kt_s). \quad (36)$$

A slightly more complex but more accurate discretization formulas to get \mathbf{A}_k and \mathbf{B}_k are given as follows [19, page 53]:

$$\mathbf{A}_k = e^{\mathbf{A}t_s}, \quad \mathbf{B}_k = \int_0^{t_s} e^{\mathbf{A}\tau} \mathbf{B}(\tau) d\tau. \quad (37)$$

4 The LQR design

Given the linearized spacecraft model (30) which has the state variables composed of spacecraft quaternion \mathbf{q} , the spacecraft rotational rate with respect to the LVLH frame $\boldsymbol{\omega}$, and the reaction wheel rotational speed $\boldsymbol{\Omega}$, we can see that to control the spacecraft attitude and to manage the reaction wheel momentum are equivalent to minimize the following objective function

$$\int_0^\infty (\mathbf{x}^T \mathbf{Q} \mathbf{x} + \mathbf{u}^T \mathbf{R} \mathbf{u}) dt \quad (38)$$

under the constraints of (30). This is clearly a LQR design problem which has known efficient methods to solve. However, in each special case, this system has some special properties which should be fully utilized to select the most efficient and effective method for each of these cases. The corresponding discrete time system is given as follows:

$$\lim_{N \rightarrow \infty} \left(\min \frac{1}{2} \mathbf{x}_N^T \mathbf{Q}_N \mathbf{x}_N + \frac{1}{2} \sum_{k=0}^{N-1} \mathbf{x}_k^T \mathbf{Q}_k \mathbf{x}_k + \mathbf{u}_k^T \mathbf{R}_k \mathbf{u}_k \right) \quad (39)$$

s.t. $\mathbf{x}_{k+1} = \mathbf{A}\mathbf{x}_k + \mathbf{B}_k\mathbf{u}_k + \mathbf{d}_k$

4.1 Case 1: $i_m = 0$

It was shown in [21] that a spacecraft without a reaction wheel in this orbit is not controllable. But for a spacecraft with three reaction wheels as we discussed in this paper, the system is fully controllable. The controllability condition can be checked straightforward but the check is tedious and is omitted in this paper (also the controllability check is not the focus of this paper). In this case, as we have seen from (30), (34), and (36) that the linear system is time-invariant. Therefore, a method for time-varying system

is not appropriate for this simple problem. For this linear time-invariant system, the optimal solution of (39) is given by (see [19, page 69])

$$\mathbf{u}_k = -(\mathbf{R} + \mathbf{B}^T \mathbf{P} \mathbf{B})^{-1} \mathbf{B}^T \mathbf{P} \mathbf{A} \mathbf{x}_k = -\mathbf{K} \mathbf{x}_k, \quad (40)$$

where \mathbf{P} is a constant positive semi-definite solution of the following discrete-time algebraic Riccati equation (DARE)

$$\mathbf{P} = \mathbf{Q} + \mathbf{A}^T \mathbf{P} \mathbf{A} - \mathbf{A}^T \mathbf{P} \mathbf{B} (\mathbf{R} + \mathbf{B}^T \mathbf{P} \mathbf{B})^{-1} \mathbf{B}^T \mathbf{P} \mathbf{A}. \quad (41)$$

There is an efficient algorithms [22] for this DARE system and an Matlab function `dare` implements this algorithm.

4.2 Case 2: $i_m \neq 0$

It was shown in [21] that a spacecraft without any reaction wheel in any orbit of this case is controllable if the spacecraft design satisfies some additional conditions imposed on \mathbf{J} matrix. By intuition, the system is also controllable by adding reaction wheels. As a matter of fact, adding reaction wheels will achieve better performance of spacecraft attitude as pointed in [1, page 19]. The best algorithm for this case is a little tricky because \mathbf{B} is a time-varying matrix but \mathbf{A} is a constant matrix. Therefore, a method for time-varying system must be used. The optimal solution of (39) is given by (see [23])

$$\mathbf{u}_k = -(\mathbf{R}_k + \mathbf{B}_k^T \mathbf{P}_{k+1} \mathbf{B}_k)^{-1} \mathbf{B}_k^T \mathbf{P}_{k+1} \mathbf{A}_k \mathbf{x}_k = -\mathbf{K}_k \mathbf{x}_k, \quad (42)$$

where \mathbf{P}_k is a periodic positive semi-definite solution of the following periodic time-varying Riccati (PTVR) equation

$$\mathbf{P}_k = \mathbf{Q}_k + \mathbf{A}_k^T \mathbf{P}_{k+1} \mathbf{A}_k - \mathbf{A}_k^T \mathbf{P}_{k+1} \mathbf{B}_k (\mathbf{R}_k + \mathbf{B}_k^T \mathbf{P}_{k+1} \mathbf{B}_k)^{-1} \mathbf{B}_k^T \mathbf{P}_{k+1} \mathbf{A}_k. \quad (43)$$

Hench and Laub [24] developed an efficient algorithm for solving the general PTVR equation. However, since $\mathbf{A}_k = \mathbf{A}$ is a constant matrix, their algorithm is not optimized. A more efficient algorithm in this case was recently proposed in [13], which is particularly useful for time-varying system with long period and a constant \mathbf{A} matrix because it may save hundreds of matrix inverses. The algorithm is presented below (its proof is in [13]):

Algorithm 4.1

Data: i_m , \mathbf{J} , \mathbf{J}_w , \mathbf{Q} , \mathbf{R} , the altitude of the spacecraft (for the calculation of a in (32)), t_s (the selected sample time period), and p (the total samples in one period $P = \frac{2\pi}{\omega_0}$).

Step 1: For $k = 1, \dots, p$, calculate \mathbf{A}_k and \mathbf{B}_k using (36) or (37).

Step 2: Calculate \mathbf{E}_k and \mathbf{F}_k using

$$\mathbf{E}_k = \begin{bmatrix} \mathbf{I} & \mathbf{B}_k \mathbf{R}^{-1} \mathbf{B}_k^T \\ \mathbf{0} & \mathbf{A}^T \end{bmatrix}, \quad (44)$$

$$\mathbf{F}_k = \begin{bmatrix} \mathbf{A} & \mathbf{0} \\ -\mathbf{Q} & \mathbf{I} \end{bmatrix} = \mathbf{F}. \quad (45)$$

Step 3: Calculate $\mathbf{\Gamma}_k$, for $k = 1, \dots, p$, using

$$\mathbf{\Gamma}_k = \mathbf{F}^{-1} \mathbf{E}_k \mathbf{F}^{-1} \mathbf{E}_{k+1} \dots \mathbf{F}^{-1} \mathbf{E}_{k+p-2} \mathbf{F}^{-1} \mathbf{E}_{k+p-1}. \quad (46)$$

Step 4: Use Schur decomposition

$$\begin{bmatrix} \mathbf{W}_{11k} & \mathbf{W}_{12k} \\ \mathbf{W}_{21k} & \mathbf{W}_{22k} \end{bmatrix}^T \mathbf{\Gamma}_k \begin{bmatrix} \mathbf{W}_{11k} & \mathbf{W}_{12k} \\ \mathbf{W}_{21k} & \mathbf{W}_{22k} \end{bmatrix} = \begin{bmatrix} \mathbf{S}_{11k} & \mathbf{S}_{12k} \\ \mathbf{0} & \mathbf{S}_{22k} \end{bmatrix}. \quad (47)$$

Step 5: Calculate \mathbf{P}_k using

$$\mathbf{P}_k = \mathbf{W}_{21k} \mathbf{W}_{11k}^{-1} \quad (48)$$

Remark 4.1 This algorithm makes full use of the fact that \mathbf{A} is a constant matrix in (45). Therefore, \mathbf{F} is a constant matrix and the inverse of \mathbf{F} in (46) does not need to be repeated many times which is the main difference between the method in [13] and the method in [24] (where $\mathbf{E}_k = \mathbf{E}$ is a constant matrix but \mathbf{F}_k is a series of time varying matrices and inverse has to take for every \mathbf{F}_k with $k = 1, \dots, p$).

Remark 4.2 The proposed method can easily be extended to the case of using momentum wheel where the speed of the flywheel is desired to be a non-zero constant. Let $\bar{\boldsymbol{\Omega}}$ be the desired speed of the momentum wheels and $\bar{\mathbf{x}} = [\mathbf{0}^T, \bar{\boldsymbol{\Omega}}^T, \mathbf{0}^T]^T$. The objective function of (38) should be revised to

$$\int_0^\infty [(\mathbf{x} - \bar{\mathbf{x}})^T \mathbf{Q} (\mathbf{x} - \bar{\mathbf{x}}) + \mathbf{u}^T \mathbf{R} \mathbf{u}] dt. \quad (49)$$

5 Simulation test

Our simulation has several goals. First, we would like to show that the proposed design achieves both attitude control and reaction wheel momentum management. Second, we would like to compare with the design [13] which does not use reaction wheels, our purpose is to show that using reaction wheels achieves better attitude pointing accuracy. More important, we would like to demonstrate that the LQR design works very well for attitude and desaturation control for the nonlinear spacecraft in the environment close to the reality. Finally, we will discuss the strategy in real spacecraft control system implementation.

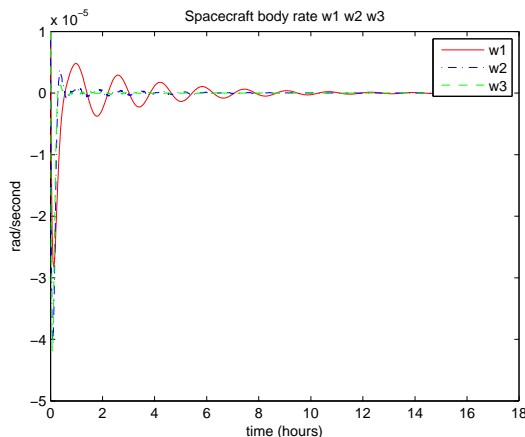


Figure 1: Body rate response ω_1 , ω_2 , and ω_3 .

5.1 Comparison with the design without reaction wheels

The proposed design algorithm has been tested using the same spacecraft model and orbit parameters as in [13] with the spacecraft inertia matrix given by

$$\mathbf{J} = \text{diag}(250, 150, 100) \text{ kg} \cdot \text{m}^2.$$

The orbital inclination $i_m = 57^\circ$ and the orbit is assumed to be circular with the altitude 657 km. In view of equation (31), the orbital period is 5863 seconds and the orbital rate is $\omega_0 = 0.0011$ rad/second. Assuming that the total number of samples taken in one orbit is 100, then, each sample period is 58.6352 second. It is easy to see that all parameters are selected the same as [13] so that we can compare the two different designs. Select $\mathbf{Q} = \text{diag}([0.001, 0.001, 0.001, 0.001, 0.001, 0.001, 0.02, 0.02, 0.02])$ and

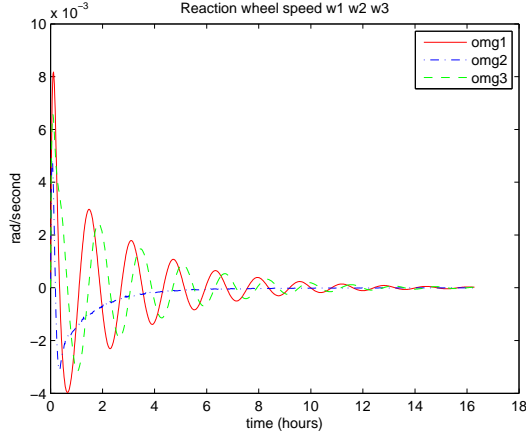


Figure 2: Reaction wheel response Ω_1 , Ω_2 , and Ω_3 .

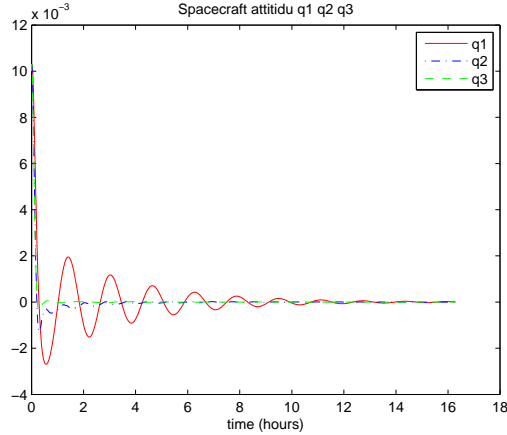


Figure 3: Attitude response q_1 , q_2 , and q_3 .

$\mathbf{R} = \text{diag}([10^3, 10^3, 10^3, 10^2, 10^2, 10^2])$. We have calculated and stored \mathbf{P}_k for $k = 0, 1, 2, \dots, 99$ using Algorithm 4.1. Assuming that the initial quaternion error is $(0.01, 0.01, 0.01)$, initial body rate vector is $(0.00001, 0.00001, 0.00001)$ radians/second, and the initial wheel speed vector is $(0.00001, 0.00001, 0.00001)$ radians/second, applying the feedback (42) to the linearized system (30) and (33), we get the linearized spacecraft rotational rate response described in Figure 1, the reaction wheel response described in Figure 2, and the spacecraft attitude responses given in Figures 3.

Comparing the response obtained here using both reaction wheels and magnetic torque coils and the response obtained in [13] that uses magnetic torques only, we can see that both control methods stabilize the spacecraft, but using reaction wheels achieve much accurate nadir pointing. Also reaction wheel speeds approach to zero as t goes to infinity. Therefore, the second design goal for reaction wheel desaturation is achieved nicely.

5.2 Control of the nonlinear system

It is nature to ask the following question: can the designed controller (42), which is based on the linearized model, stabilize the original nonlinear spacecraft system (21) with satisfied performance? We answer this question by applying the designed controller to the original nonlinear spacecraft system (21). More specifically, the LVLH frame rotational rate $\boldsymbol{\omega}_{lvlh}^b$ is calculated using the accurate nonlinear formula (12) not the approximated linear model (22). The gravity gradient torque \mathbf{t}_g is calculated using the

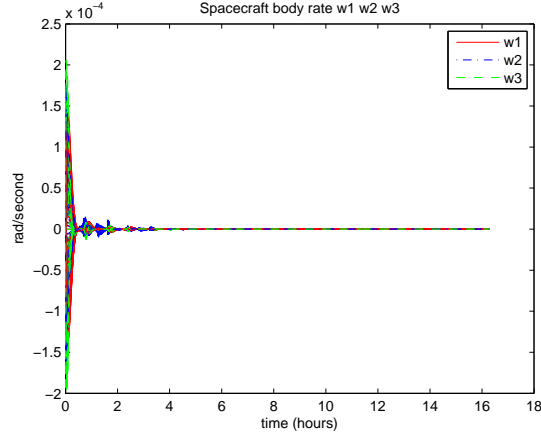


Figure 4: Body rate response ω_1 , ω_2 , and ω_3 .

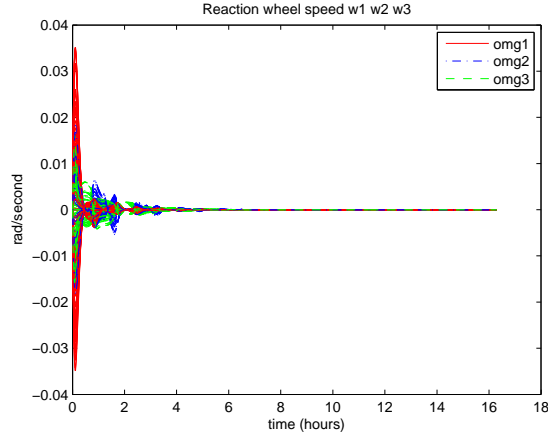


Figure 5: Reaction wheel response Ω_1 , Ω_2 , and Ω_3 .

accurate nonlinear formula (16) not the approximated linear model (23). The Earth’s magnetic field is calculated using the much accurate International Geomagnetic Reference Field (IGRF) model [26] not the simplified model (32). This is done as follows. Given the altitude of the spacecraft (657 km), the orbital radius R is 7028 kilo meters and the lateral speed of the spacecraft is $v = R\omega_0$ [2, page 109]. Assuming that the ascending node at $t = 0$ (“now”) is the \mathbf{X} axis of the ECEF frame, the velocity vector $\mathbf{v} = [0, v \cos(i_m), v \sin(i_m)]^T$. Using Algorithm 3.4 of [25, page 142], we can get the spacecraft coordinate in ECI frame at any time after $t = 0$. Converting ECI coordinate to ECEF coordinate, we can calculate a much accurate Earth magnetic field vector \mathbf{b} using IGRF model [26], which has been implemented in Matlab. Applying this Earth magnetic field vector \mathbf{b} and feedback control $\mathbf{u}_k = -\mathbf{K}_k \mathbf{x}_k$ designed by the LQR method to (21), we control the nonlinear spacecraft system using the LQR controller. Also, we allow randomly generated larger initial errors (possibly 10 time large than we used in the previous simulation test) in this simulation test.

The nonlinear spacecraft system response to the LQR controller is given in Figures 4, 5, and 6. These figures show that the proposed design does achieve our design goals. Moreover, the difference between the linear (approximate) system response and nonlinear (true) system response for the LQR design is very small!

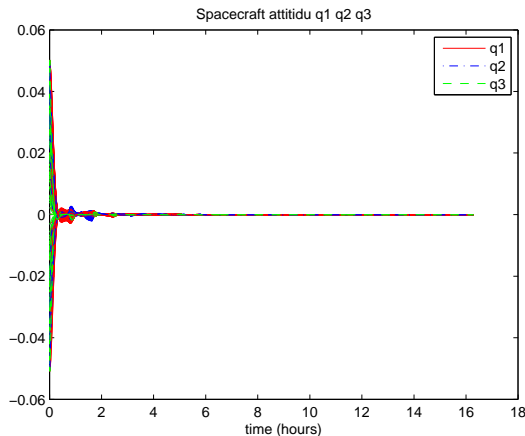


Figure 6: Attitude response q_1 , q_2 , and q_3 .

5.3 Implementation to real system

In real space environment, even the magnetic field vector obtained from the high fidelity IGRF model may not be identical to the real magnetic field vector which can be measured by magnetometer installed on spacecraft. Therefore, it is suggested to use the measured magnetic field vector \mathbf{b} to form \mathbf{B}_k in the state feedback (42). Because of the interaction between the magnetic torque coils and the magnetometer, it is a common practice that measurement and control are not taken at the same time (some time slot in the sample period is allocated to the measurement and the rest time in the sample period is allocated for control). Therefore, a scaling for the control gain should be taken to compensate for the time loss in the sample period when measurement is taken. For example, if the magnetic field measurement uses half time of the sample period, the control gain should be doubled because only half sample period is used for control. This is similar to the method used in [27].

6 Conclusions

In this paper, we developed a reduced quaternion spacecraft model which includes gravity gradient torque, geomagnetic field along the spacecraft orbit and its interaction with the magnetic torque coils, and the reaction wheels. We investigate a time-varying LQR design method to control the spacecraft attitude to align the body frame with the local vertical local horizontal frame and to desaturate the reaction momentum at the same time. A periodic optimal controller is proposed for this purpose. The periodic controller design is based on an efficient algorithm for the periodic time-varying Riccati equations. Simulation test is given to show that the design objective is achieved and the control system using both reaction wheels and magnetic torques accomplishes more accurate attitude than the control system using only magnetic torques.

References

- [1] Wertz, J. Spacecraft Attitude Determination and Control, Kluwer Academic Publishers, Dordrecht, Holland, 1978.
- [2] Sidi, M.J. Spacecraft Dynamics and Control: A Practical Engineering Approach, Cambridge University Press, Cambridge, UK, 1997.
- [3] Silani E. and Lovera M. Magnetic spacecraft attitude control: a survey and some new results, Control Engineering Practice, 13, pp. 357-371, 2005.

- [4] Rodriguez-Vazouez, A. Martin-Prats, M. A. and Bernelli-Zazzera F. Spacecraft magnetic attitude control using approximating sequence Riccati equations, *IEEE transactions on Aerospace and Electronic Systems*, 51(4), pp. 3374-3385, 2015.
- [5] Dzielsk, J. Bergmann E. and Paradiso J. A computational algorithm for spacecraft control and momentum management, *Proceedings of the 1990 American Control Conference*, pp. 1320-1325, 1990.
- [6] Chen X. Steyn, W. H. Hodgart, S. and Hashida, Y. Optimal combined reaction-wheel momentum management for Earth-pointing satellites, *Journal of guidance, control, and dynamics*, 22(4), pp. 543-550, 1999.
- [7] Giuliatti, F. Quarta, A. A. and Tortora, P. Optimal control laws for momentum-wheel desaturation using magnetorquers, *Journal of guidance, control, and dynamics*, 29(6), pp. 1464-1468, 2006.
- [8] Trequet, J-F. Arzelier, D. Peaucelle, D. Pittet, C. and Zaccarian, L. Reaction wheel desaturation using magnetorquers and static input allocation, *IEEE Transactions on Control System Technology*, 23(2), pp. 525-539, 2015.
- [9] de Angelis, E.L. Giuliatti, F. de Ruiter, A.H.J. and Avanzini, G. Spacecraft attitude control using magnetic and mechanical actuation, to appear in *Journal of Guidance, Control, and Dynamics*.
- [10] Yang, Y. Quaternion based model for momentum biased nadir pointing spacecraft, *Aerospace Science and Technology*, 14(3), pp. 199-202, 2010.
- [11] Flamm, D.S. A new shift-invariant representation for periodic linear system, *Systems and Control Letters*, 17(1), pp. 9-14, 1991.
- [12] Khargonekar, P. P. Poolla, K. and Tanenbaum, A. Robust control of linear time-invariant plants using periodic compensation, *IEEE Transactions on Automatic Control*, 30 (11), pp. 1088 - 1096, 1985.
- [13] Yang, Y. An Efficient Algorithm for Periodic Riccati Equation for Spacecraft Attitude Control Using Magnetic Torques, submitted, 2016. Available in arXiv:1601.01990.
- [14] Yang, Y. Spacecraft attitude determination and control: quaternion-based method, *Annual Reviews in Control*, 36 (2), pp. 198-219, 2012.
- [15] Serway R. A. and Jewett, J. W. *Physics for Scientists and Engineers*, Books/Cole Thomson Learning, Belmont, CA, 2004.
- [16] Wie, B. *Vehicle Dynamics and Control*, AIAA Education Series, Reston, VA, 1998.
- [17] Yang, Y. Analytic LQR design for spacecraft control system based on quaternion model, *Journal of Aerospace Engineering*, 25(3), pp. 448-453, 2012.
- [18] Yang, Y. Quaternion based LQR spacecraft control design is a robust pole assignment design, *Journal of Aerospace Engineering*, 27(1), pp. 168-176, 2014.
- [19] Lewis, F.L. Vrabie, D. and Syrmos, V.L. *Optimal Control*, 3rd Edition, John Wiley & Sons, Inc., New York, USA, 2012.
- [20] Paiaki, M.L. Magnetic torque attitude control via asymptotic period linear quadratic regulation, *Journal of Guidance, Control, and Dynamics*, 24(2), pp. 386-394, 2001.
- [21] Yang, Y. Controllability of spacecraft using only magnetic torques, *IEEE Transactions on Aerospace and Electronic System*, 52(2), pp. 955-962, 2016.
- [22] Arnold, W.F., III and Laub, A.J. Generalized Eigenproblem Algorithms and Software for Algebraic Riccati Equations, *Proc. IEEE*, 72, pp. 1746-1754, 1984.

- [23] Bittanti, S. Periodic Riccati equation, *The Riccati Equation*, edited by S. Bittanti, et. al, Spriner, Berlin, pp. 127-162, 1991.
- [24] Henc, J.J. and Laub, A.J. Numerical solution of the discrete-time periodic Riccati equation, *IEEE Transactions on Automatic Control*, 39(6), pp. 1197-1210, 1994.
- [25] Curtis, H. D. *Orbital Mechanics for Engineering Students*, Elsevier Butterworth-Heinemann, Burlington, MA, 2005.
- [26] Finlay, C.C. et al, Special issue “International geomagnetic reference field-the twelfth generation”, *Earth, Planets and Space*, 67:158, 2015.
- [27] Yang, Y. Attitude control in spacecraft orbit-raising using a reduced quaternion model, *Advances in Aircraft and Spacecraft Science*, Vol. 1, No. 4 (2014) pp. 427-441.